Molecular ion implanter equipped with liquid-metal alloy ion source

Y. Gotoh,[a] H. Tsuji, and J. Ishikawa
Department of Electronic Science and Engineering, Kyoto University, Yoshida-honmachi, Sakyo-ku, Kyoto 606-8501, Japan

(Presented on 6 September 1999)

Molecular ion implanter was developed with a liquid-metal alloy ion source. Use of a liquid-metal alloy ion source enables us to generate various kinds of molecular ions. To apply liquid-metal ion source to a general ion implanter, it is necessary to converge the divergent beam. We adopted the lens system we have already developed, and examined its performance by computer simulation and experiments. An example of molecular ion implantation was demonstrated with gold-antimony ion source. 24 keV $AuSb^{2+}$ was implanted into silicon, and presence of gold and antimony atoms was confirmed by Rutherford backscattering spectrometry and particle induced x-ray emission measurements. © *2000 American Institute of Physics.* [S0034-6748(00)58902-3]

I. INTRODUCTION

Liquid-metal ion sources (LMISs) have been utilized almost only for focused ion beam techology,[1] but they have many attractive features as a general metal ion source: simple structure, low power consumption, and no gas flow which is compatible to ultrahigh vacuum systems. Thus, various kinds of application is expected including materials science. A LMIS produces not only singly charged monomer ions, but also doubly charged monomer ions, as well as doubly charged molecular ions. We have developed gold-antimony (Au–Sb) ion sources[2] and found that intense molecular ions of $Au_mSb_n^{k+}$ were produced. Especially, the intensity of $AuSb^{2+}$ reached about 10% of total ion current and almost half of the most dominant ion species, Au^+. The fraction of the molecular intensity did not change with an increase in the emission current.[3] Other alloy ion sources also yield intense molecular ions.[4] Production of molecular ions is one of the unique feature of the ion source whose ionization mechanism is based on the surface effect.

On the other hand, molecular implantation was performed with homogeneous molecules such as N_2 and O_2, or hydrides of boron, phosphine and arsenic.[5] Also decaborane[6] implantation attracted much interest for formation of a shallower junction. We have proposed molecular ion implantation which emphasizes the introduction of heterogeneous atoms into solids.[7] This molecular ion implantation has two advantages: introduction of different elements to similar depth at a single implantation, and simultaneous implantation at the same position. However, we did not demonstrate any typical example because production of heterogeneous molecular ion is generally difficult. However, as stated above, using LMIS, it becomes possible. Combination of Au and Sb might make a metallized layer and *n*-type semiconductor junction with very thin region. The present article deals with the performance of a molecular ion implanter equipped with a LM alloy ion source.

[a]Electronic mail: ygotoh@kuee.kyoto-u.ac.jp

II. PERFORMANCE OF ION IMPLANTER WITH LIQUID-METAL ION SOURCE

A. Configuration of ion implanter

One of the most significant difficulties to apply a LMIS to an ion implanter, is how to converge the divergent beam. We have already developed the ion beam transport system.[8,9] The present implantation system was a slightly modified version, as shown in Fig. 1. In this system, divergent beam is converged by a source lens, and later again adjusted the focal length to match the mass separator by a postlens. The source lens, which is illustrated as an insert of Fig. 1, consists of three electrodes, which compose physically asymmetric lens. The extracted ion beam is converged by this lens at the early stage of its divergence. The source lens can form almost a parallel beam. However, beamlets close to beam envelop have shorter focal length due to spherical aberration, thus excess focusing is not preferred. Furthermore, focusing just after extraction gives large image magnification, so it is necessary to use another lens system. In the present study, cylindrical einzel lens with the inner diameter of 80 mm was used as a postlens. In the previous system, einzel lens with the inner diameter of 60 mm was set just after the source lens.[9] The mass separator was a sector magnet with the deflection angle of 60°, and the radius of the curvature of 600 mm.

B. Evaluation of optics

We estimated the optical performance of the implanter. As described above, after passing through the source lens, each beamlet no longer has the same object point due to spherical aberration. The trajectory for each beamlet within the source lens was calculated by trajectory calculation based on the numerical integration of equation of motion. The potential distribution within the lens were calculated by finite difference method. The entrance aperture of the present source lens allows the beam upto the divergent half angle of 25°, thus 15 beamlets including on axis beam was analyzed. In order to simplify the analysis, radially emitted beam was assumed at the entrance of the source lens. The potentials of

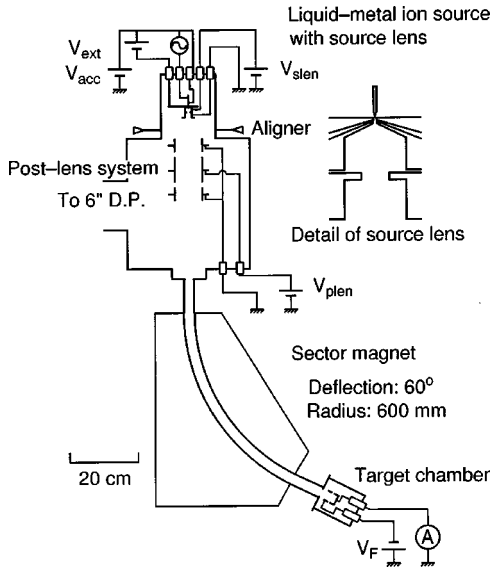

FIG. 1. Schematic diagram of ion implanter.

ion emitter, extraction electrode, center lens electrode, and last electrode were 20 kV, 12 kV, 18 kV, and 0 V. The outer 5 beamlets hit the lens electrode and 10 beamlets passed the source lens. We assumed the ion beam includes energy spread of ±100 eV.

From the above calculation, we obtain the radial position and the component of radial velocity of each beamlet. Since the beam diameter is less than 10 mm, we can treat the following optical elements with the first order approximation. The focal point of each beamlet was calculated using a given characteristics published as a table.[10] Transport matrix of sector magnet was also given in the literature.[11]

Figures 2(a)–2(d) show the phase space diagram for the ion beam at the various point of the implanter. Figures 2(a)–2(d) are those at the exit of the source lens, just in front of the postlens, just in front of the mass separator, and at the exit of the mass separator. The initial beam is slightly diverging, but after passing through the postlens, the beam is formed to be almost parallel. The 10 beamlets which passed through the source lens could be transported to the target. Based on the radial current distribution of In ion source at the source current of 200 μA, the current is almost 38 μA. We have obtained the current of approximately 40 μA with Ga ion source, which agrees well to the present result.

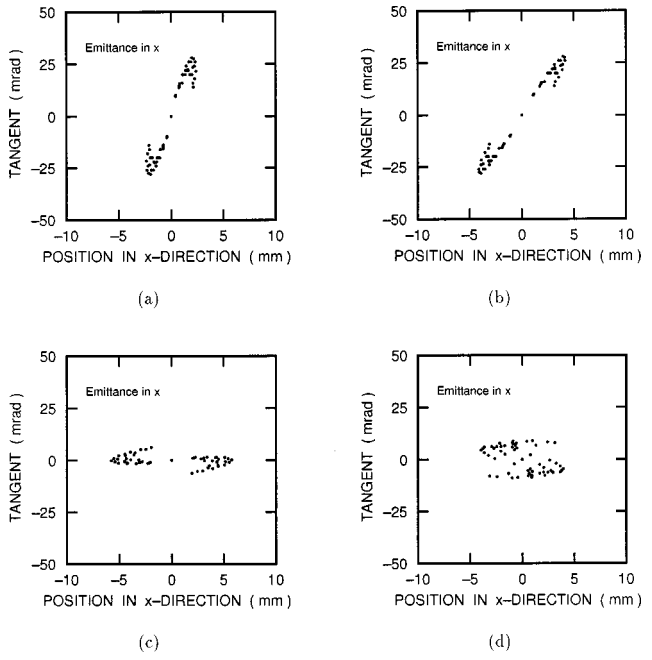

FIG. 2. Phase space diagram of the ion beam at various points of the implanter. (a) At the exit of the source lens, (b) at the entrance of postlens, (c) at the entrance of mass separator, and (d) at the exit of mass separator.

TABLE I. Condition of molecular ion implantation.

Terms	Conditions
Ion species	$AuSb^{2+}$
Ion energy	24 keV
Ion current	0.6 μA, equivalent to 0.2 μA cm^{-2}
Ion dose	6.7×10^{15} ions cm^{-2}
Substrate	*n*-Si(100)
Ion incident angle	7° off with respect to substrate normal

C. Separation of molecules

The ion species which appear close to the $AuSb^{2+}$(mass/charge=160) was Sb^{+}(mass/charge=122), and Sb_3^{2+}(mass/charge=183). $\Delta m/m$'s are 0.24 and 0.14, which can be well separated by the present mass separator. If $AuSb^{+}$ is used, Au_3^{2+}(mass/charge=295.5) and $AuSb_4^{2+}$ (mass/charge=342.5) appear close to $AuSb^{+}$(mass/charge =319) thus separation of these ions is difficult.

III. MOLECULAR IMPLANTATION

A. Sample preparation

Molecular ion implantation was performed with the $AuSb_2$ ion source.[2] As described above, use of $AuSb^{2+}$ is preferred to avoid cross contamination of different molecules. We implanted with the condition written in Table I. The ion current during implantaion was 0.6 μA. Taking the fraction of $AuSb^{2+}$ ions in the total beam current (7.4%), transported current was 8.1 μA, if we assume the ion beam consists of a single ion species. This value is lower than the above calculated values, and it would be attributed both to low angular intensity growth for Au–Sb ion source[3] and to lower acceleration voltage of 12 kV.

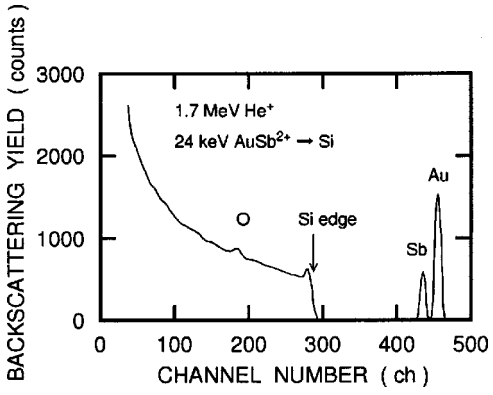

FIG. 3. RBS spectrum of the molecular ion implanted sample.

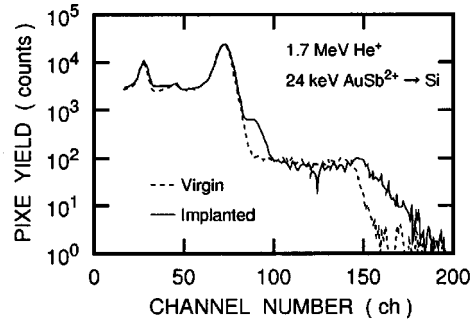

(a)

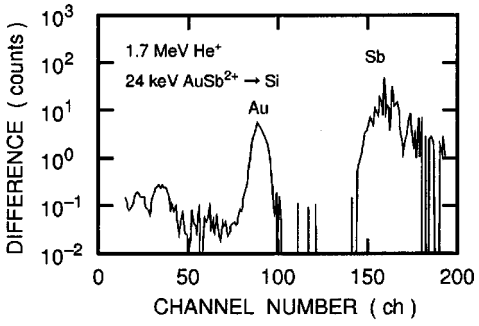

(b)

FIG. 4. PIXE spectrum of molecular ion implanted sample. (a) Signals from implanted sample and virgin substrate and (b) difference of two signals normalized by virgin signal.

B. Analysis of implanted sample

In order to confirm the presence of the implanted atoms, characterization of implanted sample was performed. Figures 3 and 4 indicate the spectra of Rutherford backscattering spectrometry (RBS) and particle induced x-ray emission (PIXE) measurements, respectively. The probe beam was 1.7 MeV He^+ and scattering angle was 135°. From the RBS spectrum, two peaks due to heavy atoms can be seen. The positions of these peaks well agree with those for Au and Sb. Peak area ratio of Sb/Au was 0.40 which showed good agreement with the theoretical value of 0.42.[12] The absolute implanted dose could not be confirmed because the RBS spectrum shows chanelling effect of the substrate silicon, but considered to be within an error of 50%. Further confirmation was performed by PIXE. Figure 4(a) shows the raw data obtained from the implanted and virgin samples. Only a slight difference could be seen, and the difference was enhanced by subtracting the virgin signal from the implanted signal. The difference was normalized by the virgin singal. This result is shown in Fig. 4(b). The peak at the lower energy corresponds to Au $M\alpha$ 2.12 keV, and that at the higher energy corresponds to Sb $L\alpha$ 3.60 keV.[13] From these measuremnts, simultaneous implantation of both Au and Sb was confirmed.

IV. SUMMARY

Molecular ion implanter equipped with a liquid-metal alloy ion source is proposed and a fundamental result on the molecular ion implantation was demonstrated. $AuSb^{2+}$ was implanted into a silicon substrate, and the presence of Au and Sb atoms were confirmed by RBS and PIXE.

ACKNOWLEDGMENT

The RBS and PIXE measurements were performed at Quantum Science and Engineering Center, Kyoto University.

[1] J. Orloff, Rev. Sci. Instrum. **64**, 1105 (1993).
[2] Y. Gotoh, H. Tsuji, and J. Ishikawa, Jpn. J. Appl. Phys., Part 1 **35**, 3670 (1996).
[3] Y. Gotoh, H. Tsuji, and J. Ishikawa, Ultramicroscopy **73**, 83 (1998).
[4] W. M. Clark, Jr., R. L. Seliger, M. W. Utlaut, A. E. Bell, L. W. Swanson, G. A. Schwind, and J. B. Jergenson, J. Vac. Sci. Technol. B **5**, 197 (1987).
[5] A. Yoshida, M. Kitagawa, and T. Hirao, Jpn. J. Appl. Phys., Part 1 **32**, 2151 (1993).
[6] D. Takeuchi, N. Shimada, J. Matsuo, and I. Yamada, Nucl. Instrum. Methods Phys. Res. B **121**, 345 (1997).
[7] J. Ishikawa, H. Tsuji, M. Mimura, and Y. Gotoh, IEEE Proceedings of the 11th International Conference on Ion Implantation Technology, Austin, 1996 (unpublished), p. 776.
[8] J. Ishikawa, Y. Gotoh, H. Tsuji, and T. Takagi, Nucl. Instrum. Methods Phys. Res. B **21**, 186 (1987).
[9] J. Ishikawa, H. Tsuji, T. Kashiwagi, and T. Takagi, Nucl. Instrum. Methods Phys. Res. B **37/38**, 155 (1989).
[10] A. B. El-Kareh and J. C. J. El-Kareh, *Electron Beams, Lenses, and Optics* (Academic, Orlando, FL, 1970).
[11] R. G. Wilson and G. R. Brewer, *Ion Beams, With Application To Ion Implantation* (Krieger, Malabar, 1979).
[12] W.-K. Chu, J. W. Mayer, and M.-A. Nicolet, *Backscattering Spectrometry* (Academic, Orlando, FL, 1978).
[13] I. V. Mitchell and J. F. Ziegler, *Ion Induced X-Rays*, edited by J. W. Mayer and E. Rimini, Ion Beam Handbook of Material Analysis (Academic, New York, 1977), Chap. 5, p. 311.